Heterostructure Barrier Varactor Simulation Using an Integrated Hydrodynamic Device/Harmonic-Balance Circuit Analysis Technique

J. R. Jones, *Student Member, IEEE*, S. H. Jones, *Member, IEEE*, G. B. Tait, *Member, IEEE*, and M. F. Zybura

Abstract— **Accurate and efficient simulations of the large-signal time-dependent behavior of GaAs/AlGaAs Heterostructure Barrier Varactor (HBV) frequency tripler circuits have been obtained. This is accomplished by combining a novel harmonic-balance circuit analysis technique with a physics-based hydrodynamic device simulator. The integrated HBV hydrodynamic device/harmonic-balance circuit simulator allows HBV multiplier circuits to be co-designed from both a device and a circuit point of view. Comparisons are made with the experimental results of Choudhury *et al.* for GaAs/AlGaAs HBV frequency triplers operating near 200 GHz. These comparisons illustrate the importance of representing active devices with physics-based numerical device models rather than analytical device models based on lumped quasi-static equivalent circuits.**

I. Introduction

THE development of highly nonlinear circuits such as large-signal amplifiers, frequency converters, and oscillators requires the use of a harmonic-balance circuit analysis technique to adequately characterize the interaction between the nonlinear device and its linear embedding circuit. Typically, the nonlinear device is analytically modelled by a lumped quasi-static equivalent circuit. The use of such a model, however, has limited validity at high device operating frequencies, requires significant insight into the operation of the nonlinear device in order to develop an equivalent circuit topology, and requires a laborious and often non-unique procedure to determine the elements of the equivalent circuit as functions of bias and frequency. An alternate approach is to utilize a physics-based numerical device model in conjunction with a harmonic-balance circuit analysis technique. Although such an approach is limited by the required computer resources and computation times, the continuing advancement of computer workstations makes it an attractive one.

In this letter, we apply this approach to the analysis of a Heterostructure Barrier Varactor (HBV)[1] frequency tripler operating near 200 GHz. The HBV, first proposed in 1989 [1], has received considerable attention as a promising device for high efficiency frequency multiplication in the millimeter-to-submillimeter wavelength range because of its attractive device characteristics and large degree of design flexibility. The structural symmetry of the HBV yields a device with an evenly symmetric nonlinear capacitance-voltage (C-V) relationship about zero DC bias. The evenly symmetric device C-V characteristic eliminates the even harmonic components from the output current waveform so that high efficiency frequency multiplier circuits, which do not require DC bias and which require fewer idlers than standard Schottky varactor multipliers, can be realized.

A DC and large-signal time-dependent hydrodynamic device simulator has been developed to analyze generic InGaAs/InP/InAlAs on InP and GaAs/InGaAs/AlGaAs on GaAs HBV's [2], [3]. The simulator is based on a physical model that combines electron transport through the heterostructure bulk with electron transport across the abrupt heterointerfaces in a fully self-consistent manner. Given the importance of both the nonlinear device and its embedding circuit in the design of frequency multipliers, the hydrodynamic device simulator has been combined with an efficient harmonic-balance circuit analysis technique to provide an integrated computer-aided design environment for the entire HBV multiplier circuit. HBV multiplier circuits can, therefore, be co-designed from both a device and a circuit point of view by specifying the device geometry, doping profile, and alloy composition profile, as well as the parasitic device impedances and embedding impedances of the circuit. When compared to the analytical lumped quasi-static equivalent circuit models typically employed in harmonic-balance circuit simulators, it will be shown that hydrodynamic device simulators more accurately describe the dynamic high frequency nonstationary behavior of carriers in nonlinear devices subject to large-signal excitation.

II. Hydrodynamic Device Simulation Technique

Carrier transport through the bulk regions of an HBV has been described by a set of one-dimensional coupled nonlinear differential equations for electrons based on the first two moments of the Boltzmann transport equation and Poisson's equation. The resulting equations governing DC and time-dependent transport are

Manuscript received August 2, 1994. J. R. Jones is supported by a USAF Laboratory Graduate Fellowship under the sponsorship of the Solid-State Directorate, Wright Laboratory, WPAFB, OH. This work is also partially supported by NSF Grants ECS-9113123 and ECS-9202037.

J. R. Jones, S. H. Jones, and M. F. Zybura are with Department of Electrical Engineering, University of Virginia, Charlottesville, VA 22903 USA.

G. B. Tait is with Department of Electrical Engineering and Computer Science, United States Military Academy, West Point, NY 10996 USA.

IEEE Log Number 9406698.

[1] Originally called the Quantum Barrier Varactor (QBV) and often called the Single Barrier Varactor (SBV), we prefer to call the device the Heterostructure Barrier Varactor (HBV) to avoid confusion with the Schottky Barrier Varactor and to emphasize the importance of the heterostructure alloy composition and doping profiles in the design and operation of the device.

$$\frac{\partial n(x,\,t)}{\partial t} = \frac{1}{q}\frac{\partial J_n(x,\,t)}{\partial x}, \tag{1}$$

$$J_n(x,\,t) = -\frac{q^2\tau_p(x)n(x,\,t)}{m^*(x)}\frac{\partial \phi_n(x,\,t)}{\partial x}, \tag{2}$$

and

$$\frac{\partial}{\partial x}\left[\epsilon(x)\frac{\partial \psi(x,\,t)}{\partial x}\right] = q[n(x,\,t) - N_D(x)], \tag{3}$$

where

$$n(x,\,t) = n_{i,\,ref}\exp\left[\frac{q}{kT}(\psi(x,\,t) + V_n(x) - \phi_n(x,\,t))\right] \tag{4}$$

and where J_n is the electron particle current density, n is the electron density, ϕ_n is the electron quasi-Fermi potential, ψ is the electrostatic potential, k is Boltzmann's constant, q is the electron charge, T is the absolute temperature, $n_{i,\,ref}$ is the intrinsic electron density in the reference material (GaAs or InP), and V_n, τ_p, m^*, N_D, and ϵ are the spatially-dependent alloy potential [4], momentum relaxation time, electron conductivity effective mass, donor impurity concentration, and dielectric permittivity, respectively.

In order to accurately model the current in heterostructure devices, careful consideration of carrier transport across abrupt material discontinuities is required [5], [6]. As such, electron transport across the abrupt heterointerfaces of an HBV has been described by a set of nonlinear electron particle current density equations that take into account thermionic emission and thermionic-field emission of carriers over and through the abrupt barrier [6]. Regardless of bias polarity, one of the two heterointerfaces in a single barrier HBV is biased above flat-band. Thus, the semiconductor-semiconductor heterointerface analog [2], [3] to the boundary constraint of Adams and Tang [7], [8] for metal-semiconductor interfaces at high forward bias has been utilized. Continuity of the electric displacement, electrostatic potential, and electron particle current density complete the set of interface conditions required for a self-consistent solution at a given heterointerface.

In order to develop a robust hydrodynamic device simulator that could be efficiently combined with a harmonic-balance circuit analysis technique, careful consideration has been given to developing a hydrodynamic device simulator with excellent numerical convergence and accuracy properties. Potential problems and inefficiencies have been minimized by the use of a finely subdivided, nonuniform mesh structure, a fully implicit finite difference time discretization scheme, and the state variables J_n, ϕ_n, ψ, and D. The four resulting carrier transport equations are solved, in the three regions (one barrier and two modulation) of the device, at a given bias value and are subject to the heterointerface constraints and ideal ohmic contact boundary constraints via the coupled equation Newton-Raphson method. In order to derive an entire I-V curve or time-domain current waveform, as well as to obtain information about the internal physics of the device as a function of bias, the DC or time-dependent bias is incrementally changed from the zero-bias condition. Multiple barrier HBV's are modelled in an ideal fashion so that only one single-barrier HBV active region is simulated with a terminal voltage equal to the total terminal voltage divided by the number of barriers.

III. Harmonic-Balance Circuit Analysis Technique

The novel harmonic-balance circuit analysis technique employed in this work is derived from the multiple-reflection algorithm [9]. The time-domain current through the device active region is calculated by the hydrodynamic device simulator, for one period, as described in the previous section. The harmonic components of the current are extracted from the time-domain current waveform using a discrete fourier transform; 13 harmonics plus the DC term have been utilized in this work. A fixed-point iterative expression, derived from the robust multiple-reflection algorithm, is then used to update the total voltage applied directly across the active region of the device in terms of the embedding impedances of the circuit, the harmonic components of the current, and the harmonic components of the voltage from previous iterations. This iterative process continues until the harmonic components of the voltage converge to their steady-state values. Complex frequency-dependent parasitic impedances, external to the active region of the device and similar to those of [9], are included in the analysis as additional contributions to the linear device embedding circuit.

The novelty in the harmonic-balance algorithm utilized here is that in deriving the fixed-point iterative voltage update expression, we use *a priori* knowledge from Kirchhoff's voltage law that the nonlinear device impedance (parasitic plus active region impedances) will equal the negative of the linear circuit impedance for each of the undriven harmonics in the steady state. This eliminates the computationally intensive and possibly unstable Runge-Kutta numerical time-integration necessary in the original multiple-reflection algorithm [9] and allows us to calculate complex under-relaxation parameters for each harmonic component of the fixed-point iterative voltage update equation. A Steffenson numerical acceleration scheme for iterative equations, derived from the secant methods of numerical analysis [10], is also utilized to greatly increase the computational speed and convergence properties of the harmonic-balance circuit analysis. Unlike Newton-type techniques, the laborious numerical calculations needed to assemble Jacobian matrices and solve large linear systems of equations are avoided, while a convergence rate nearly equal to that of Newton-type methods is maintained.

IV. Results and Discussion

Excellent correlation has been obtained between the HBV hydrodynamic device simulator and the experimental I-V and C-V results of Choudhury *et al.* [11] for single-barrier GaAs/AlGaAs HBV frequency triplers. The simulated GaAs/AlGaAs HBV, described in [11], has an active region consisting of a 213 Å intrinsic $Al_{0.7}Ga_{0.3}As$ barrier surrounded by 53 Å intrinsic GaAs spacer layers and 5330 Å n-type (1×10^{17} cm^{-3}) GaAs modulation layers. Parasitic impedances have been calculated using estimated chip parameters (ohmic contact resistivities of 2×10^{-6} Ω cm^2, substate thickness of 4 mil, and square chip side lengths of 250 μm) and the mesa parameters given in [11] for the n^+

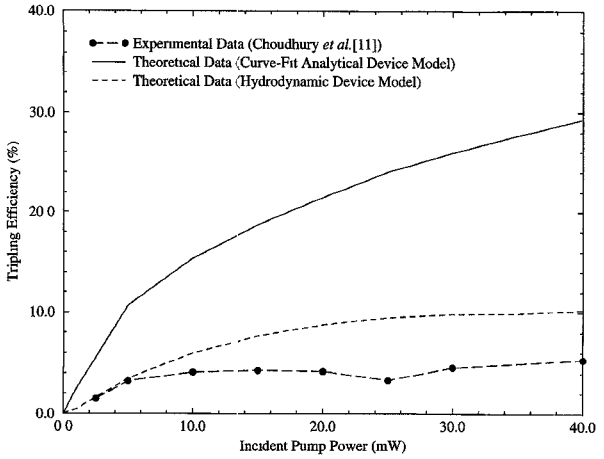

Fig. 1. Experimental and theoretical tripling efficiencies versus incident pump power for single-barrier GaAs/AlGaAs HBV's subject to 64-GHz pump excitation. Experimental results are taken from Fig. 7 of [11].

epitaxial layers external to the active region. The calculated DC parasitic resistance of 7.073 Ω compares favorably with the measured value of 7.0 Ω quoted in [11].

Results from the harmonic-balance circuit analysis, coupled to both the HBV hydrodynamic device simulator and a simple quasi-static analytical HBV device model, have been compared to the Choudhury *et al.* experimental results. The quasi-static analytical HBV device model utilizes curve fits to the device DC I-V and static C-V characteristics obtained from the HBV hydrodynamic device simulator. The total device current as an instantaneous function of bias $i(V(t))$ is, thus,

$$i(V(t)) = I_{DC}(V(t)) + C_{Static}(V(t))\frac{dV}{dt}. \qquad (5)$$

Near-optimum fundamental and third-harmonic circuit embedding impedances have been estimated from [11], at the incident pump powers of interest, for a device DC parasitic resistance of 7.0 Ω; these circuit-embedding impedances have been utilized with both simulation approaches. The remaining circuit embedding impedances have been set to short-circuit impedances ($0.001+j0.0$ Ω) for simulation purposes.

The experimental HBV tripling efficiency (*intrinsic* device efficiency) versus incident pump power data of Choudhury *et al.* is shown in Fig. 1 for a pump frequency of 64 GHz. Also shown in this figure are the simulated results obtained from the harmonic-balance circuit analysis coupled to both the analytical and numerical device models. On a Hewlett Packard Apollo 9000 Series 735 workstation, the simulations at a given pump power typically took several minutes and several hours to complete for the analytical and numerical device models, respectively. For a given incident pump power, the predicted results change very little with small variations in the fundamental and third-harmonic embedding impedances estimated from [11]; the simulated results given in Fig. 1 are, therefore, the maximum predicted efficiencies.

The simulated harmonic-balance current and voltage waveforms obtained from the two device models have the same general shape, but the sharpness, magnitudes, and phases of the waveforms differ substantially. As a result, the predicted absorbed power, third harmonic output power, and tripling efficiency are substantially overestimated by the analytical device/harmonic-balance circuit simulator. Clearly, the time-dependent behavior of electrons in HBV's is not adequately accounted for using a simple analytical device model in conjunction with the harmonic-balance circuit analysis; the dynamic high frequency nonstationary behavior of the electrons is more accurately modeled by a full numerical device model utilizing hydrodynamic transport equations.

V. Conclusions

In conclusion, accurate and efficient simulations of the large-signal time-dependent behavior of HBV's have been obtained by combining a novel harmonic-balance circuit analysis technique with a physics-based HBV hydrodynamic device simulator. Results from the harmonic-balance circuit analysis, coupled to both the HBV hydrodynamic device simulator and a simple quasi-static analytical HBV device model, have been compared to the experimental results of Choudhury *et al.* for a single barrier GaAs/AlGaAs HBV operating near 200 GHz. Favorable comparison is obtained using the integrated HBV hydrodynamic device/harmonic-balance circuit simulator. These comparisons illustrate the importance of representing active devices with physics-based numerical device models rather than analytical device models based on lumped quasi-static equivalent circuits.

Acknowledgment

The authors thank T. W. Crowe of the University of Virginia and N. R. Erickson of the University of Massachusetts for useful technical discussions relevant to this work.

References

[1] E. Kollberg and A. Rydberg, "Quantum-barrier-varactor diodes for high-efficiency millimetre-wave multipliers," *Electron. Lett.*, vol. 25, no. 25, pp. 1696–1698, Dec. 1989.

[2] J. R. Jones, G. B. Tait, and S. H. Jones, "DC and large-signal AC electron transport properties of GaAs/InGaAs/AlGaAs heterostructure barrier varactors," *Proc. 1993 Int. Semiconductor Device Research Symp.*, Charlottesville, VA, Dec. 1–3, 1993, pp. 389–392.

[3] J. R. Jones, G. B. Tait, and S. H. Jones, "DC and large-signal time-dependent electron transport in heterostructure devices: an investigation of the heterostructure barrier varactor," submitted to *IEEE Trans. Electron. Dev.*, 1994.

[4] M. S. Lundstrom and R. J. Schuelke, "Numerical analysis of heterostructure semiconductor devices," *IEEE Trans. Electron Dev.*, vol. ED-30, no. 9, pp. 1151–1159, Sept. 1983.

[5] K. Horio and H. Yanai, "Numerical modeling of heterojunctions including the thermionic emission mechanism at the heterojunction interface," *IEEE Trans. Electron Dev.*, vol. 37, no. 4, pp. 1093–1098, Apr. 1990.

[6] G. B. Tait and C. R. Westgate, "Electron transport in rectifying semiconductor alloy ramp heterostructures," *IEEE Trans. Electron Dev.*, vol. ED-38, no. 6, pp. 1262–1270, June 1991.

[7] J. G. Adams and T. W. Tang, "A revised boundary condition for the numerical analysis of schottky barrier diodes," *IEEE Electron. Dev. Lett.*, vol. ED-7, no. 9, , pp. 525–527, Sept. 1986.

[8] J. G. Adams and T. W. Tang, "Computer simulation of boundary conditions for schottky barrier diodes," *Electon. Lett.*, vol. 25, no. 16, pp. 1098–1100, Aug. 1989.

[9] P. H. Siegel, A. R. Kerr, and W. Hwang, "Topics in the optimization of millimeter-wave mixers," NASA Tech. Papers, no. 2287, Mar. 1984.

[10] J. Ortega and W. Rheinboldt, *Iterative Solution of Nonlinear Equations in Several Variables,* New York: Academic Press, 1970.

[11] D. Choudhury, M. A. Frerking, and P. D. Batelaan, "A 200 GHz tripler using a single barrier varactor," *IEEE Trans. Microwave Theory Tech.*, vol. 41, no. 4, pp. 595–599, Apr. 1993.